Silicon solar cell – Top view (showing collection grid) and cross section

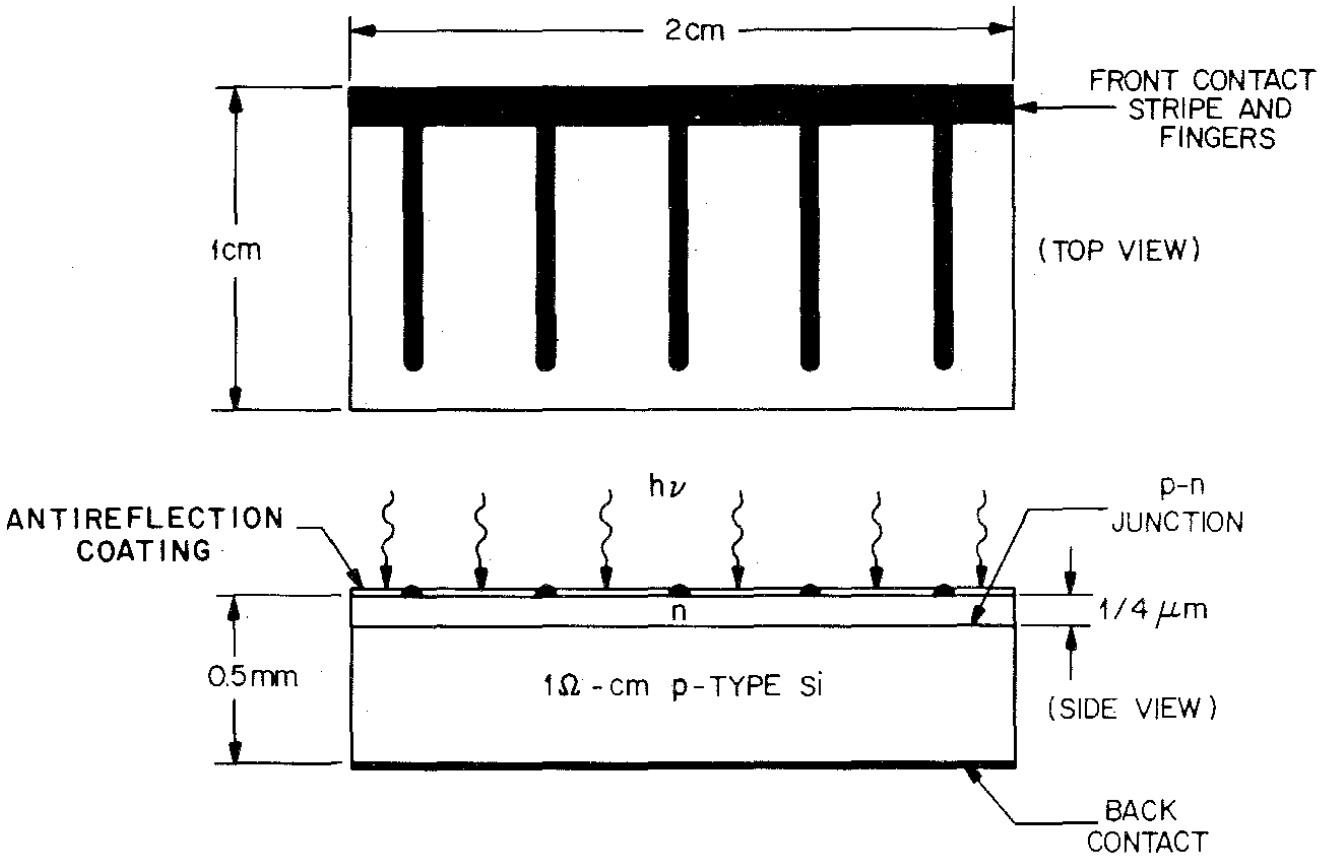

SM Sze, Physics of Semiconductor Devices, 2nd ed.

Solar Cell: a) pn junction under irradiation; b) equivalent circuit; c) IV characteristics

a) pn junction

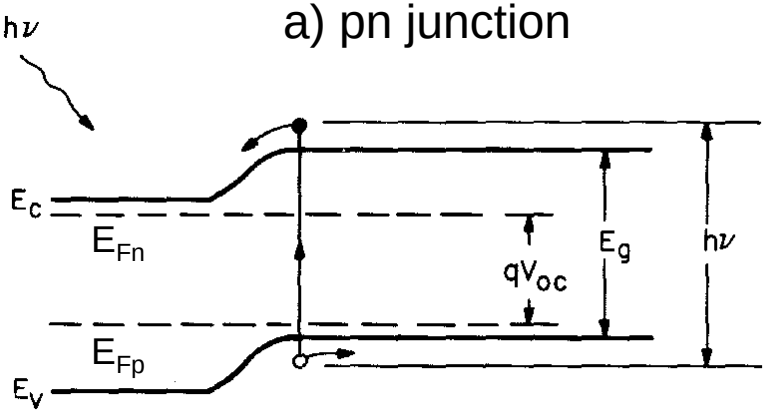

b) equivalent circuit

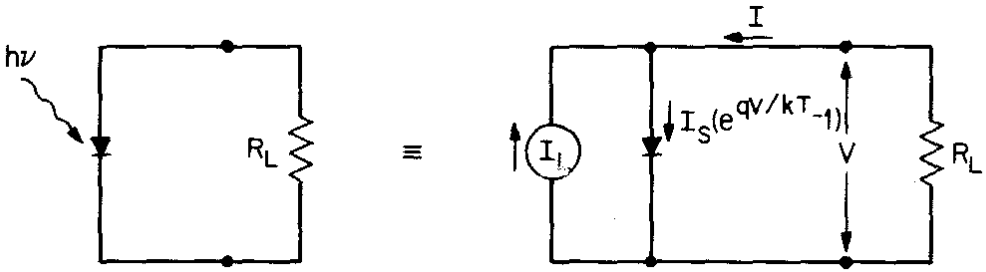

$$I = I_s(e^{qV/kT} - 1) - I_L$$

Dark current Photo current

c) IV characteristics

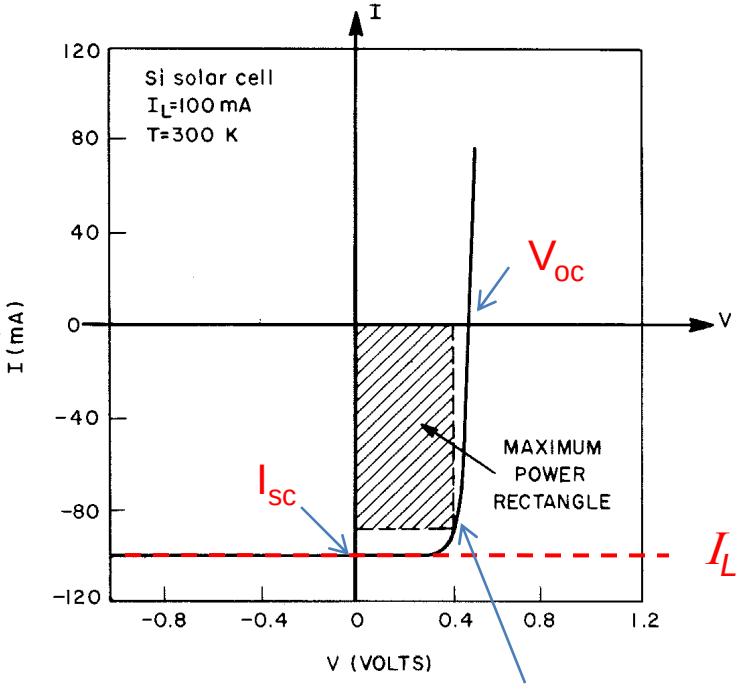

Max. power point

Power conversion efficiency = maximum power / solar power

SM Sze, Physics of Semiconductor Devices, 2nd ed.

Minority carrier lifetime, τ

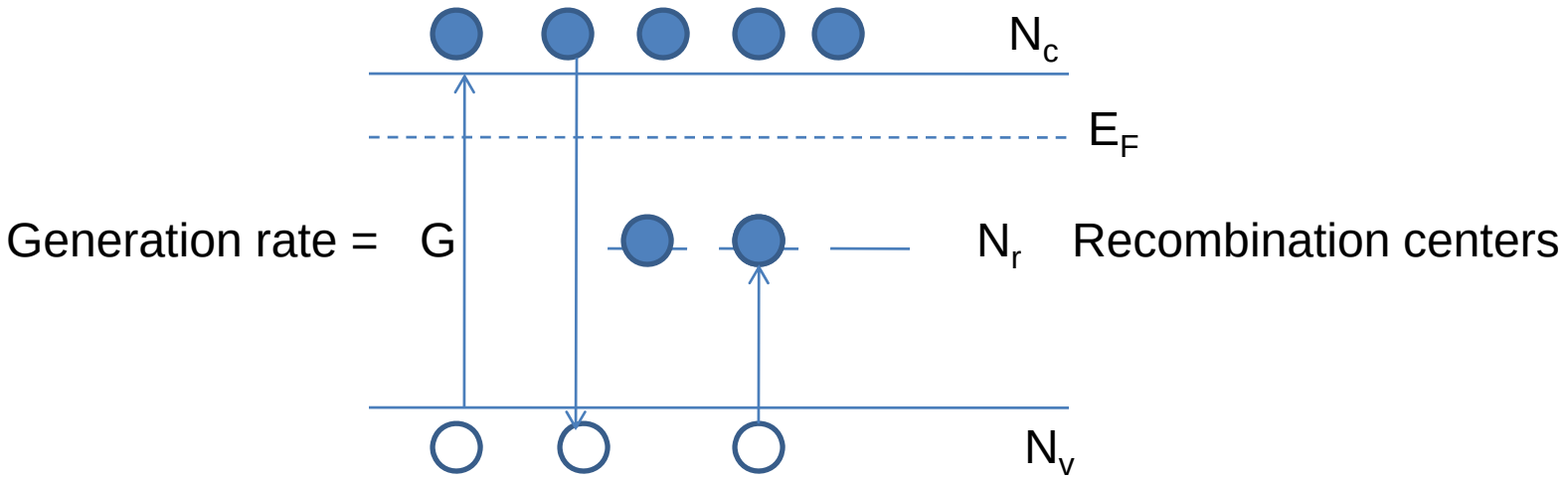

$$\tau_p = (1/\sigma_p v_{th} N_r)\left[(1+(N_c/n_{n0})\ \exp[-(E_c-E_r)/kT]) + (\sigma_p/\sigma_n)(N_V/n_{n0})\ \exp[-(E_r-E_v)/kT]\right],$$

$$\tau_{p0} = (\sigma_p v_{th} N_r)^{-1}.$$

at high doping level; n_{n0} = free electron concentration

TABLE 1
Lifetimes in Bulk Si, 300°K.
Boron-Doped Unless Otherwise Noted

ρ (ohm-cm)	Type	τ_n (10^{-6} sec)	Conditions	Ref.
10	p;FZ	55	As grown	19
		275	+ Annealed 450°C	
		10	+ Annealed 700°C	
1	p;CG	10-20	As grown	19
		20-120	+ Annealed 450°C	
1	p;FZ	110	As grown	20
		420	+ Annealed 450°C	
		15	+ Annealed 700°C	
1	p;CG	35	As grown	20
		210	+ Annealed 450°C	
		20	+ Annealed 700°C	
10	n	τ_p = 700	Li-doped, as grown	21,22
1	n	τ_p = 200	Li-doped, as grown	21,22
0.1	n	τ_p = 50	Li-doped, as grown	21,22

TABLE 3
Lifetimes and Diffusion Lengths, GaAs, 300°K

Doping (cm^{-3})	Dopant	τ_n (10^{-8} sec)	L_n (10^{-4} cm)	τ_p (10^{-8} sec)	L_p (10^{-4} cm)	Ref.
2×10^{17}	?	0.35	6-6.3	-	-	25
2×10^{18}	?	0.092	1.9-3.3	-	-	25
5×10^{18}	Zn(LPE)[a]	0.63	6	-	-	26
$>3\times10^{18}$	Zn(LPE)	>0.65	6-7	-	-	27
2×10^{18}	Zn(Boat)	0.217	4	-	-	28
1×10^{19}	Zn(Boat)	0.057	1.6	-	-	29
1×10^{18}	Ge(LPE)	5.88	23	-	-	30
5×10^{18}	Ge(LPE)	5.73	18	-	-	30
2×10^{18}	Ge(LPE)	1.50	10.5	-	-	31
1×10^{19}	Ge(LPE)	0.67	5.5	-	-	31
1×10^{17}	Ge,Sn	0.49	7.5	0.79	2.2	32
1×10^{18}	Ge,Sn	0.40	6	0.77	1.9	32
2×10^{18}	Sn	-	-	0.36	1.2	32
5×10^{18}	Ge	0.071	2	-	-	32
2×10^{17}	(Si ?)	-	-	1.9	3.1-3.5	33

[a] LPE = liquid-phase epitaxy.

Spectral Response Analysis

$G(\lambda, x)$ = generation rate ($\propto$ light intensity at distance x)

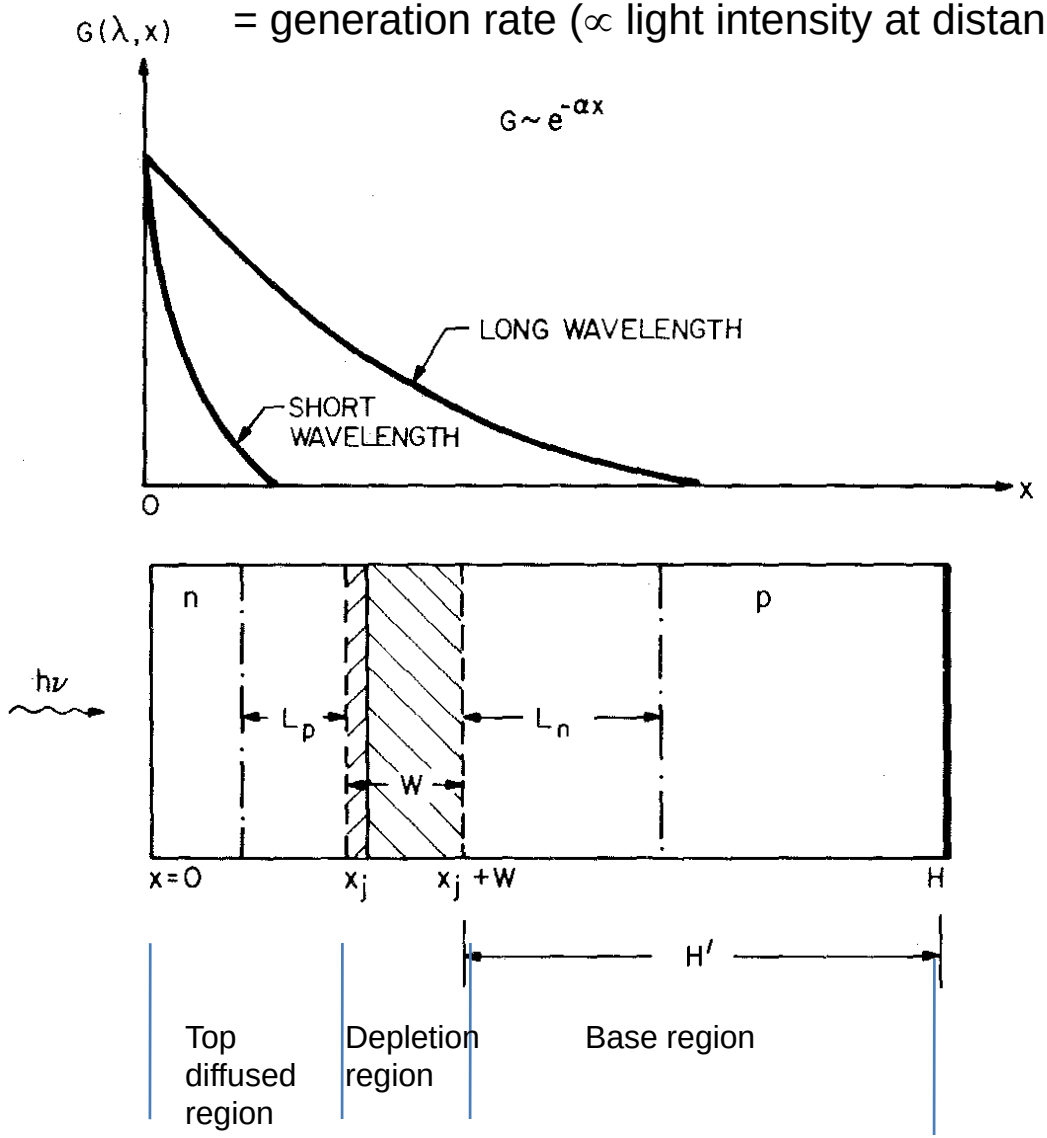

SM Sze, Physics of Semiconductor Devices, 2nd ed.

Spectral Response Analysis

Generation rate G(λ) of electron-hole pairs at distance x from the surface of a semiconductor:

$$G(\lambda) = \alpha(\lambda) F(\lambda) [1 - R(\lambda)] \exp(-\alpha(\lambda) x)$$

- $\alpha(\lambda)$: Abs. coeff.
- $F(\lambda)$: Photon flux
- $R(\lambda)$: Surface reflection
- $\exp(-\alpha(\lambda) x)$: Photon attenuation factor

$\alpha(\lambda)$ = Absorption coefficient at wavelength λ
$F(\lambda)$ = Incident photon per unit area per sec per unit bandwidth
$R(\lambda)$ = Reflection at wavelength λ

Recombination losses:

a) Bulk via recombination centers
b) Front surface via surface defects
c) Back surface via surface defects
d) Internal junction surfaces

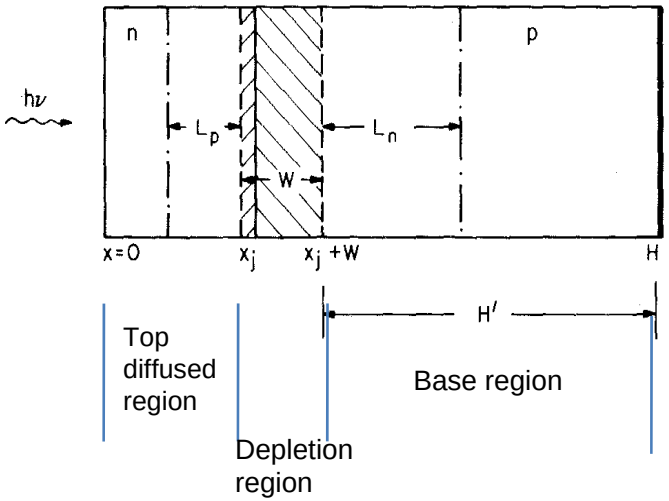

SM Sze, Physics of Semiconductor Devices, 2nd ed.

Spectral Response Analysis – contributions from top (J_p) , depletion(J_{dr}) and base (J_n) regions

$$J_p = \left[\frac{qF(1-R)\alpha L_p}{(\alpha^2 L_p^2 - 1)}\right] \times \left[\frac{\left(\frac{S_p L_p}{D_p} + \alpha L_p\right) - \exp(-\alpha x_j)\left(\frac{S_p L_p}{D_p}\cosh\frac{x_j}{L_p} + \sinh\frac{x_j}{L_p}\right)}{\frac{S_p L_p}{D_p}\sinh\frac{x_j}{L_p} + \cosh\frac{x_j}{L_p}} - \alpha L_p \exp(-\alpha x_j)\right]$$

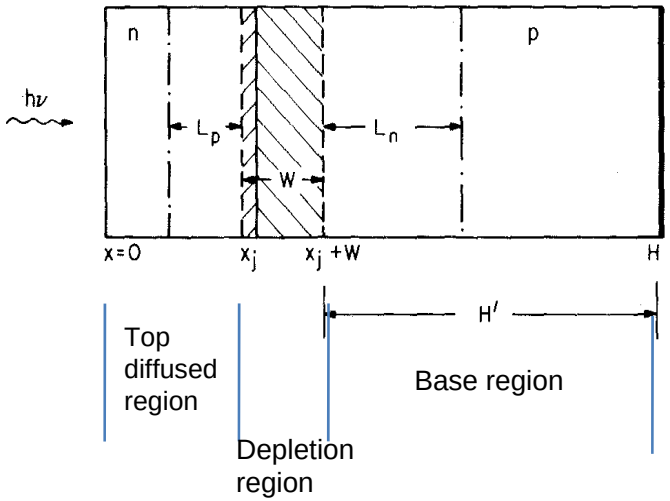

$$J_n = \frac{qF(1-R)\alpha L_n}{(\alpha^2 L_n^2 - 1)} \exp[-\alpha(x_j + W)] \times \left[\alpha L_n - \frac{\frac{S_n L_n}{D_n}\left(\cosh\frac{H'}{L_n} - \exp(-\alpha H')\right) + \sinh\frac{H'}{L_n} + \alpha L_n \exp(-\alpha H')}{\frac{S_n L_n}{D_n}\sinh\frac{H'}{L_n} + \cosh\frac{H'}{L_n}}\right]$$

$$J_{dr} = qF(1-R)\exp(-\alpha x_j)[1-\exp(-\alpha W)]$$

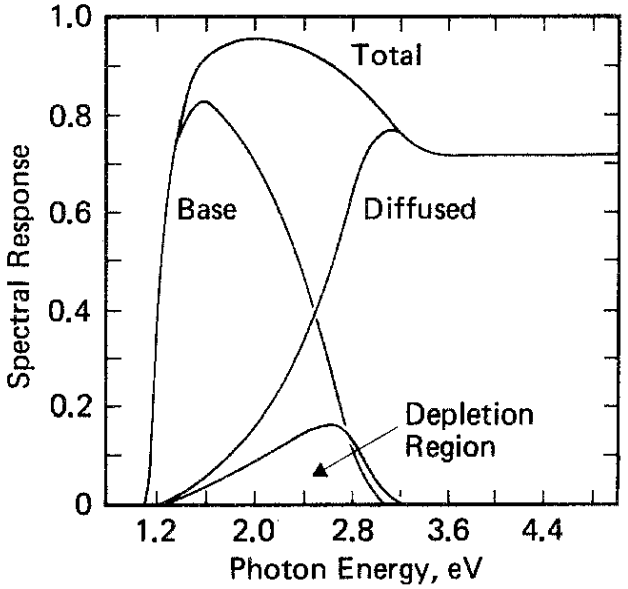

SM Sze, Physics of Semiconductor Devices, 2nd ed.

GaAs solar cell:

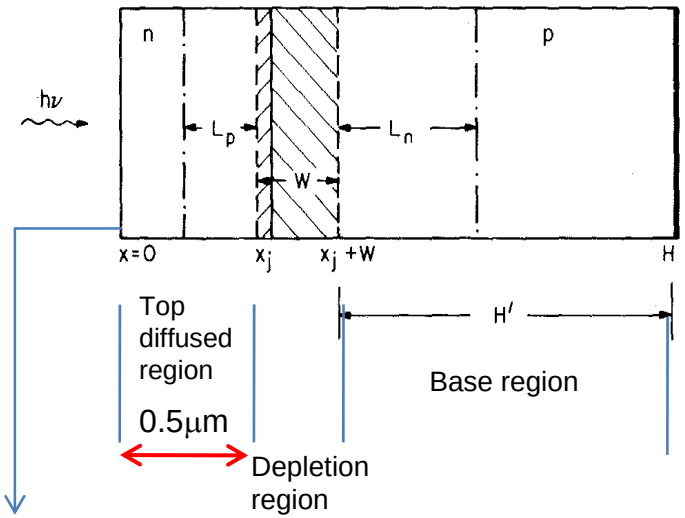

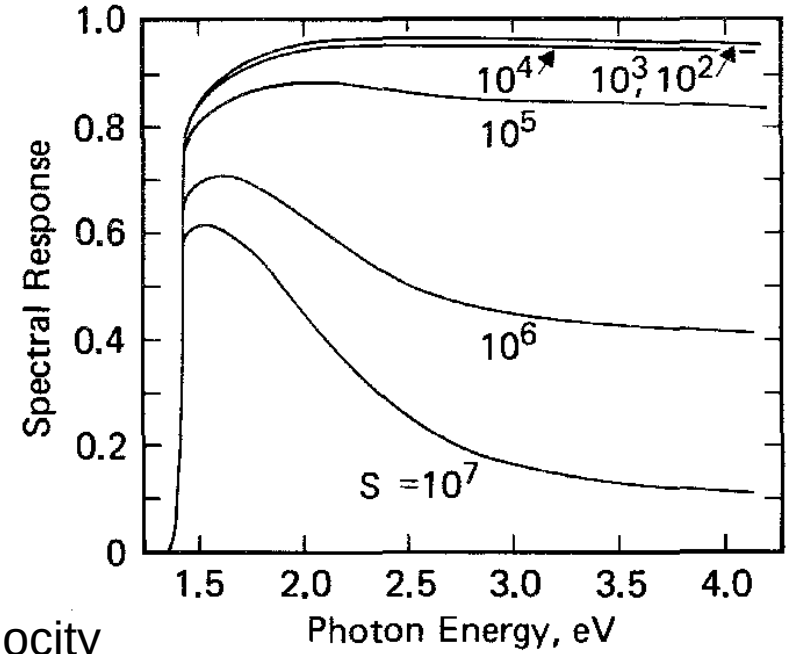

S = Front surface recombination velocity

FIG. 10. Computed internal spectral responses of GaAs P/N solar cells with uniformly doped top and base regions for various front surface recombination velocities. H = 300 μm, x_j = 0.5 μm, S_{back} = ∞. Device parameters of Table 5.

SM Sze, Physics of Semiconductor Devices, 2nd ed.

Loss at this internal surface is much reduced

p-$Ga_{1-x}Al_xAs$ / p-GaAs / n-GaAs

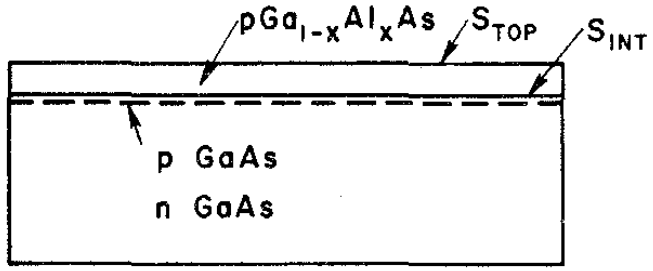

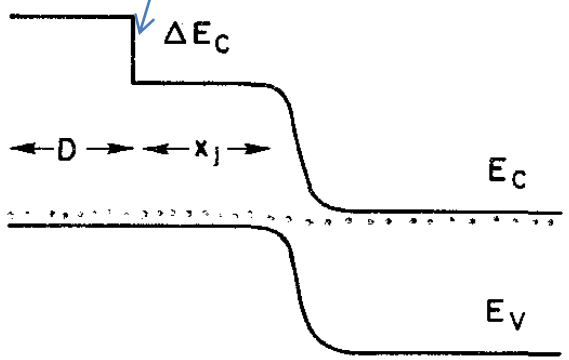

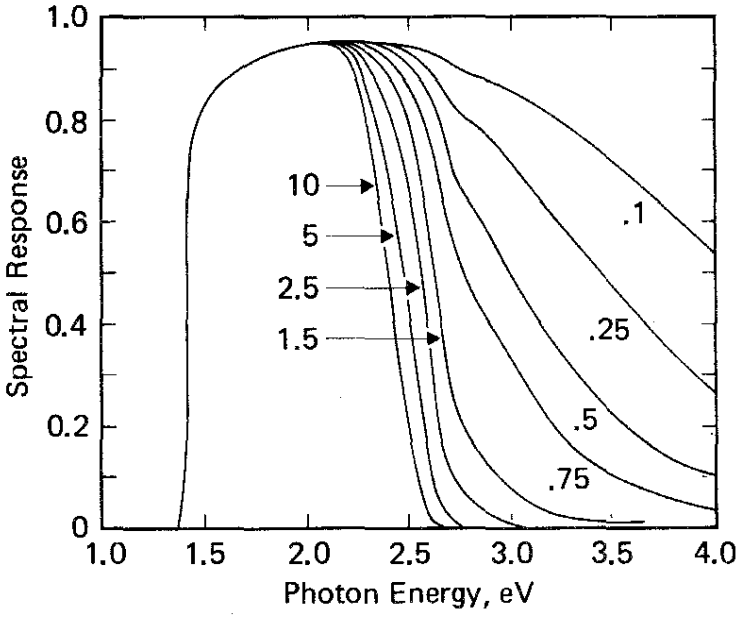

p-$Ga_{1-x}Al_xAs$ thickness dependence

FIG. 14. Computed internal spectral responses of $pGa_{1-x}Al_xAs$-pGaAs-nGaAs cells as a function of the $Ga_{1-x}Al_xAs$ thickness (in microns). Aluminum composition is 0.86. $N_a = 2\times10^{19}$ cm^{-3}, $N_d = 2\times10^{17}$ cm^{-3}, $S_{top} = 10^6$ cm/sec, $S_{interface} = 10^4$ cm/sec. $L_{top} = 0.27$ µm, $L_{pGaAs} = 1.8$ µm, $L_{nGaAs} = 3.0$ µm, $x_j = 0.5$ µm, $H = 300$ µm, $S_{back} = \infty$.

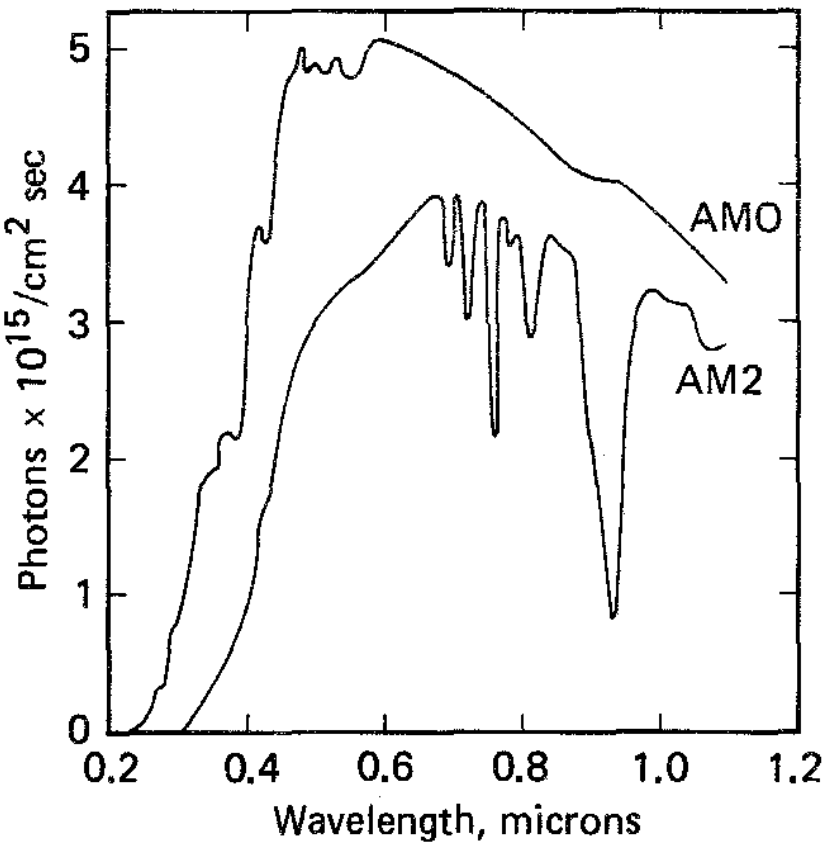

1.35kW/m^2

0.75kW/m^2

FIG. 19. Solar irradiance in photons per cm^2 per second in a 100 Å bandwidth for outer space (AM0) conditions and for average weather conditions on earth (AM2).

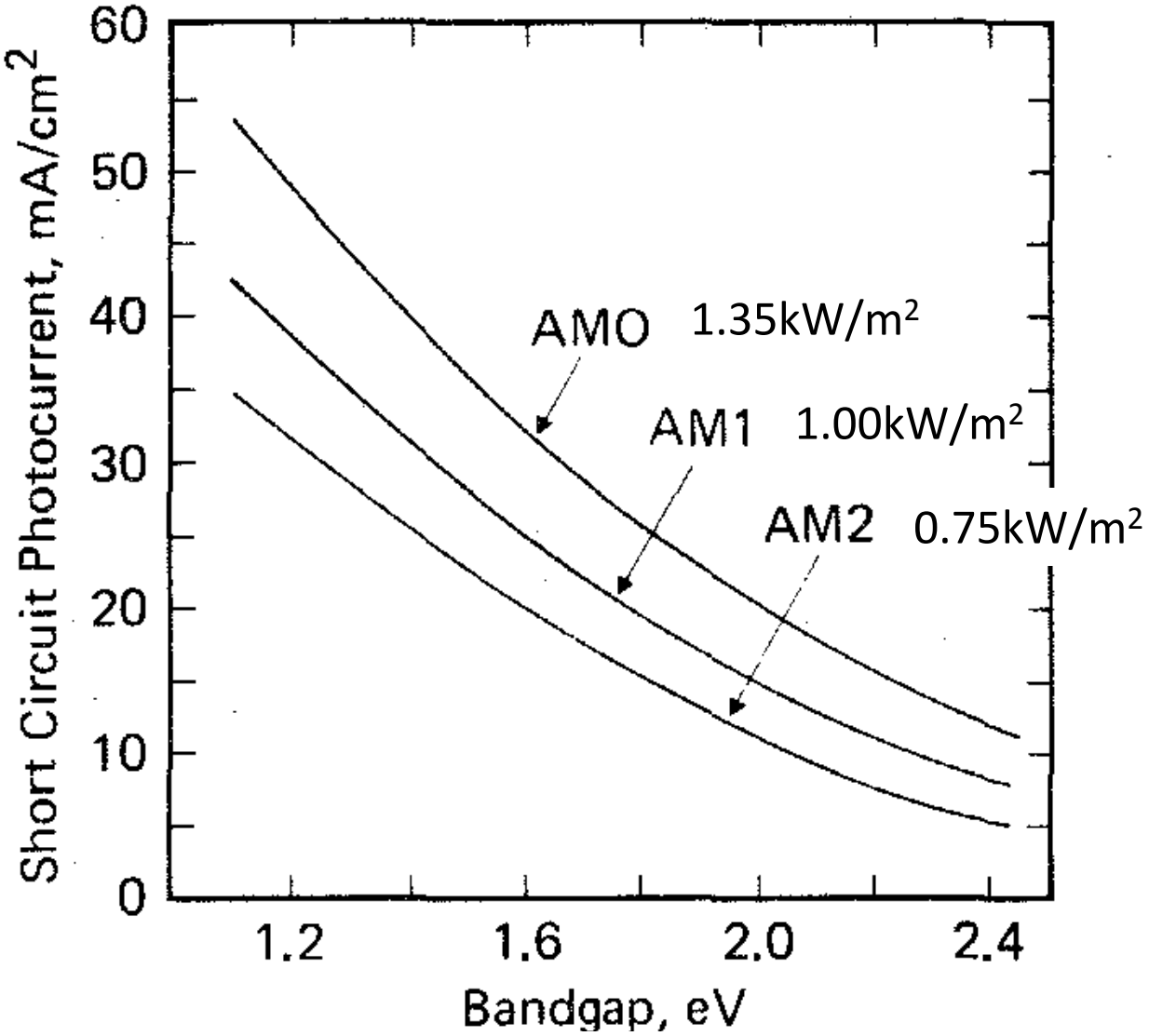

$$J_{ph} = q \int_0^{\infty} F(\lambda) SR(\lambda) \, d\lambda$$

HJ Hovel, Solar Cells

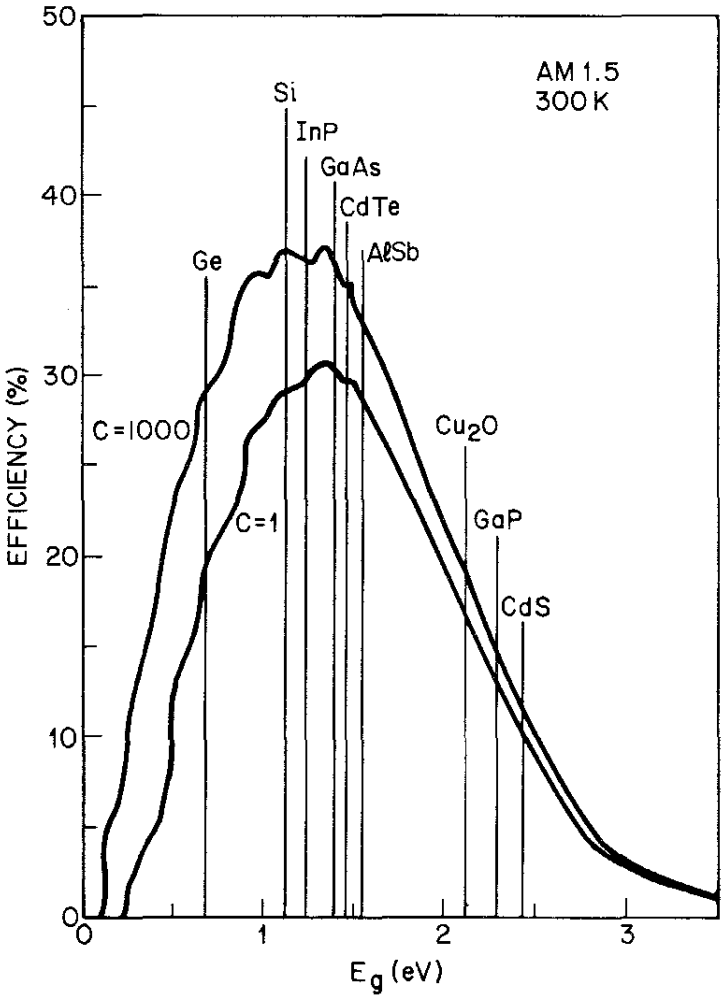

Fig. 7 Ideal solar-cell efficiency at 300 K for 1 sun and for 1000-sun concentration. (After Ref. 13.)

Silicon solar cell – Top view (showing collection grid) and cross section

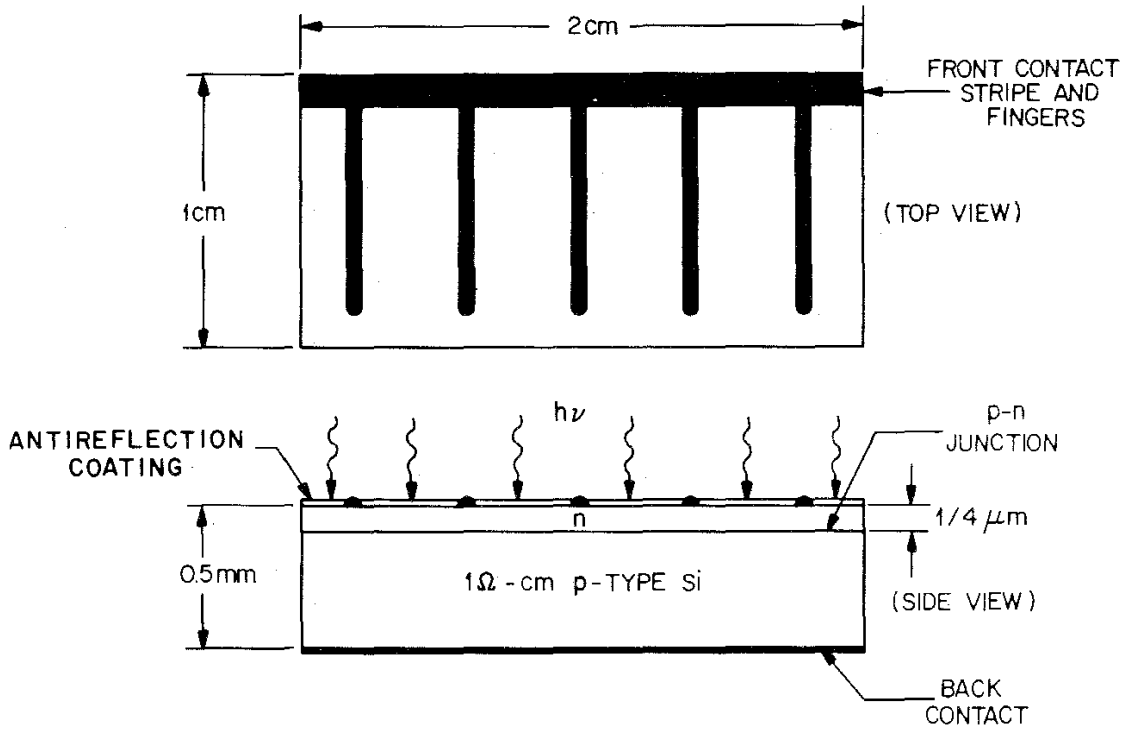

Equivalent circuit with and without series and shunt resisitances:

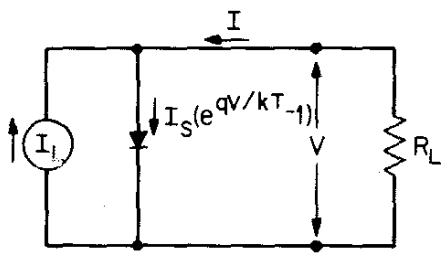

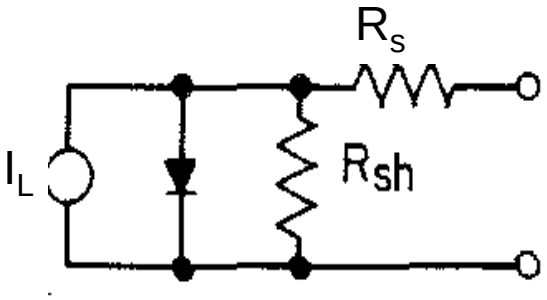

SM Sze, Physics of Semiconductor Devices, 2nd ed.

Effect of series and shunt resistances on solar cell performance:

- R_s = series resistance (from bulk, contact)
- R_{sh} = shunt resistance (from leakage, shorts)

$$I = I_s\left\{\exp\left[\frac{q(V - IR_s)}{kT}\right] - 1\right\} - I_L$$

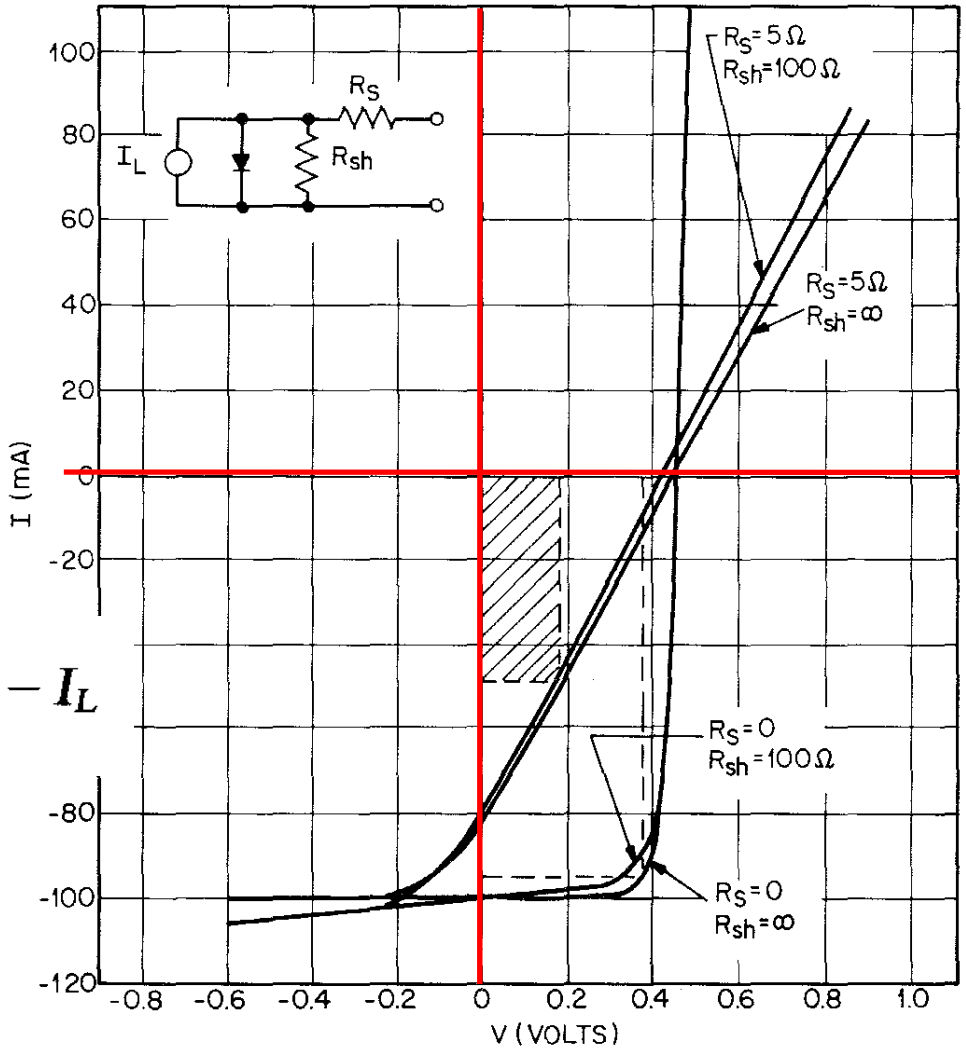

Fig. 12 Theoretical *I–V* characteristics for various solar cells that include series and shunt resistances. The insert shows the equivalent circuit. The parameters are identical to those shown in Fig. 5. (After Prince, Ref. 12.)

SM Sze, Physics of Semiconductor Devices, 2nd ed.

Back-surface field effect – reduced recombination loss at back contact; increased I_{sc} and V_{oc}

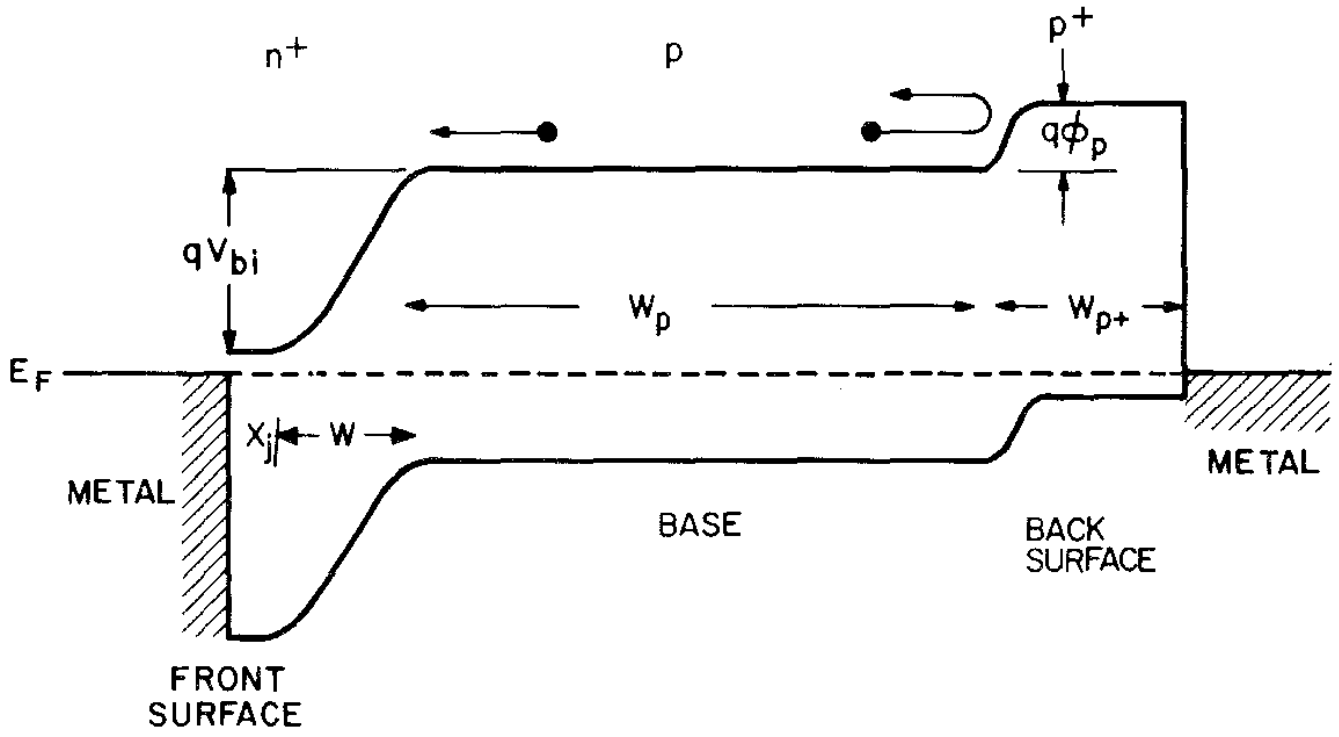

Fig. 16 Energy-band diagram for a n^+-p-p^+ back-surface field junction solar cell. (After Mandelkorn and Lamneck, Ref. 21.)

SM Sze, Physics of Semiconductor Devices, 2nd ed.

Texturized surface – increased light trapping and reduced reflection loss

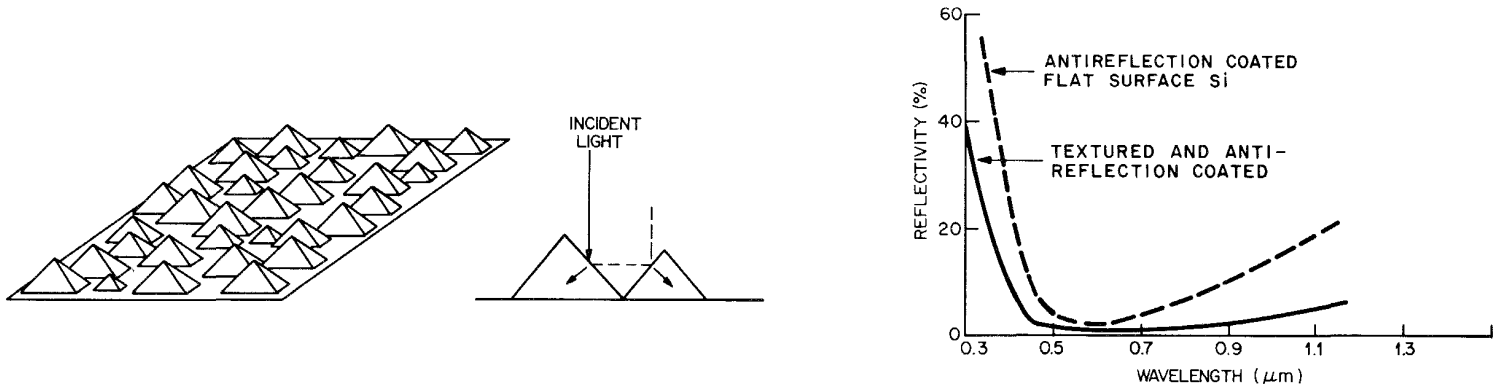

Fig. 18 (*a*) Textured cell with pyramidal surfaces. (*b*) Reflectivity versus wavelength for a flat surface cell and a textured cell. (After Arndt et al., Ref. 23.)

SM Sze, Physics of Semiconductor Devices, 2nd ed.

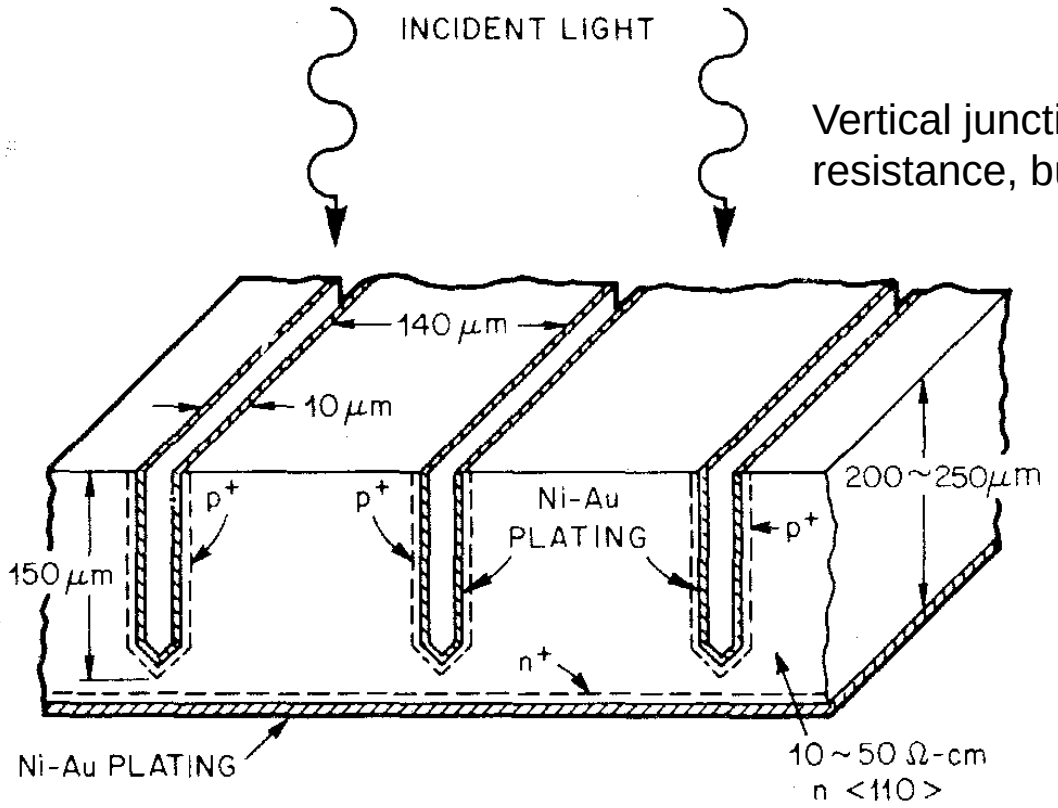

Vertical junction Si cells – reduced series resistance, but also active area

Fig. 21 Schematic diagram of low-series resistance multiple vertical-junction solar cell. (After Frank, Goodrich, and Kaplow, Ref. 26.)

SM Sze, Physics of Semiconductor Devices, 2nd ed.

Heterojunction solar cells (e.g. CdS/CdTe)

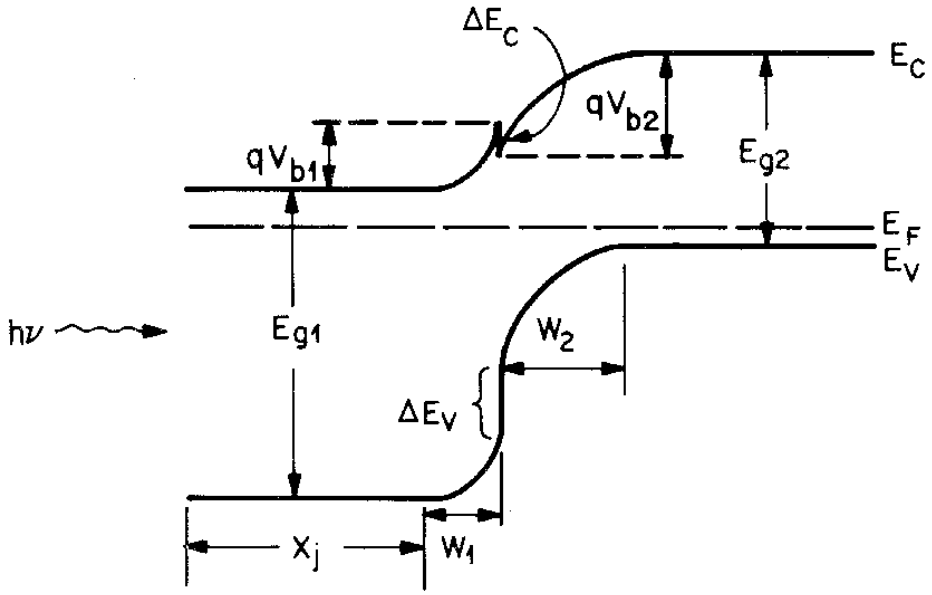

Fig. 22 Energy-band diagram of an *n*-on-*p* heterojunction in thermal equilibrium.

SM Sze, Physics of Semiconductor Devices, 2nd ed.

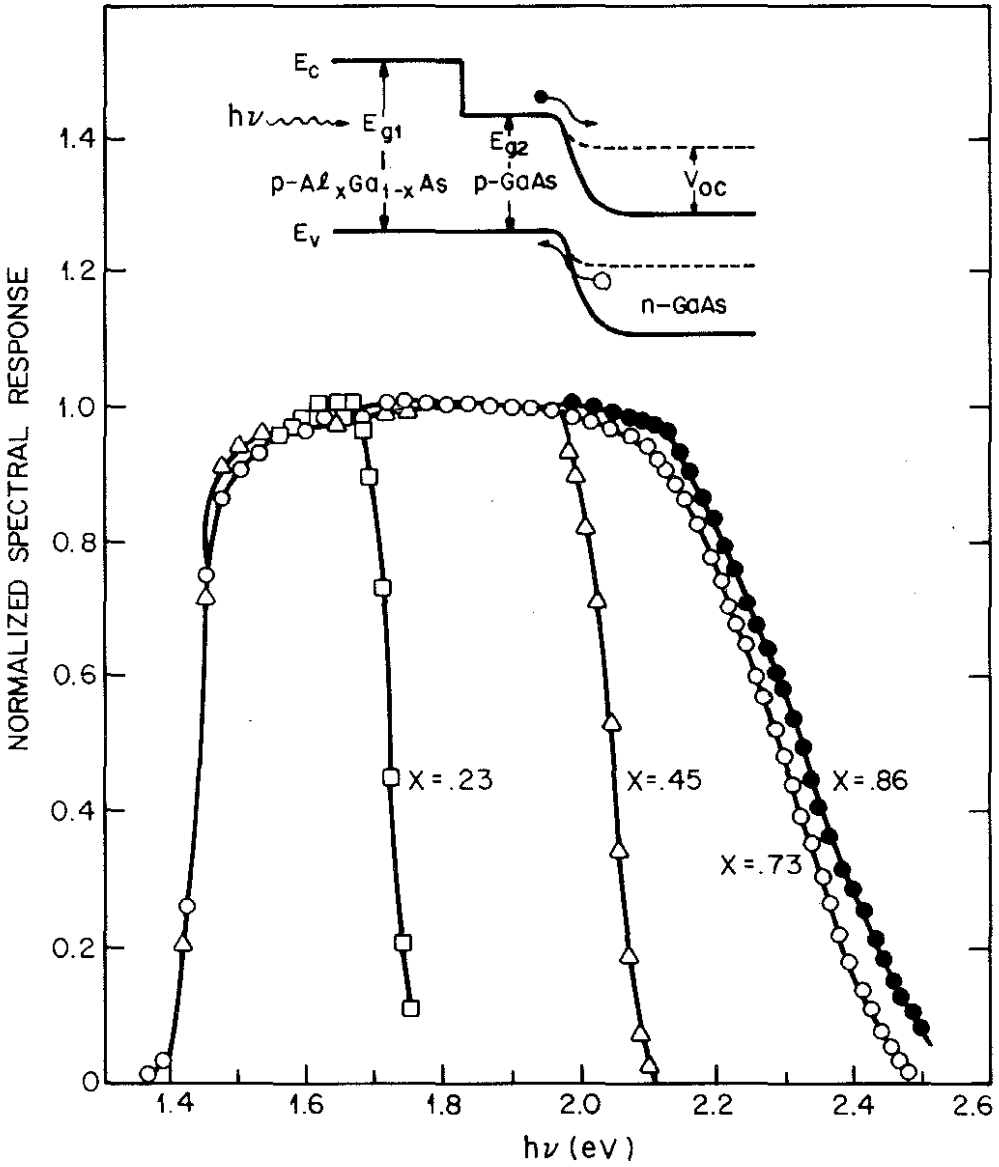

Fig. 23 Normalized spectral response for several AlGaAs/GaAs solar cells having different compositions. The insert shows the heteroface solar-cell band diagram. (After Hovel and Woodall, Ref. 28.)

SM Sze, Physics of Semiconductor Devices, 2nd ed.

Tandem solar cells

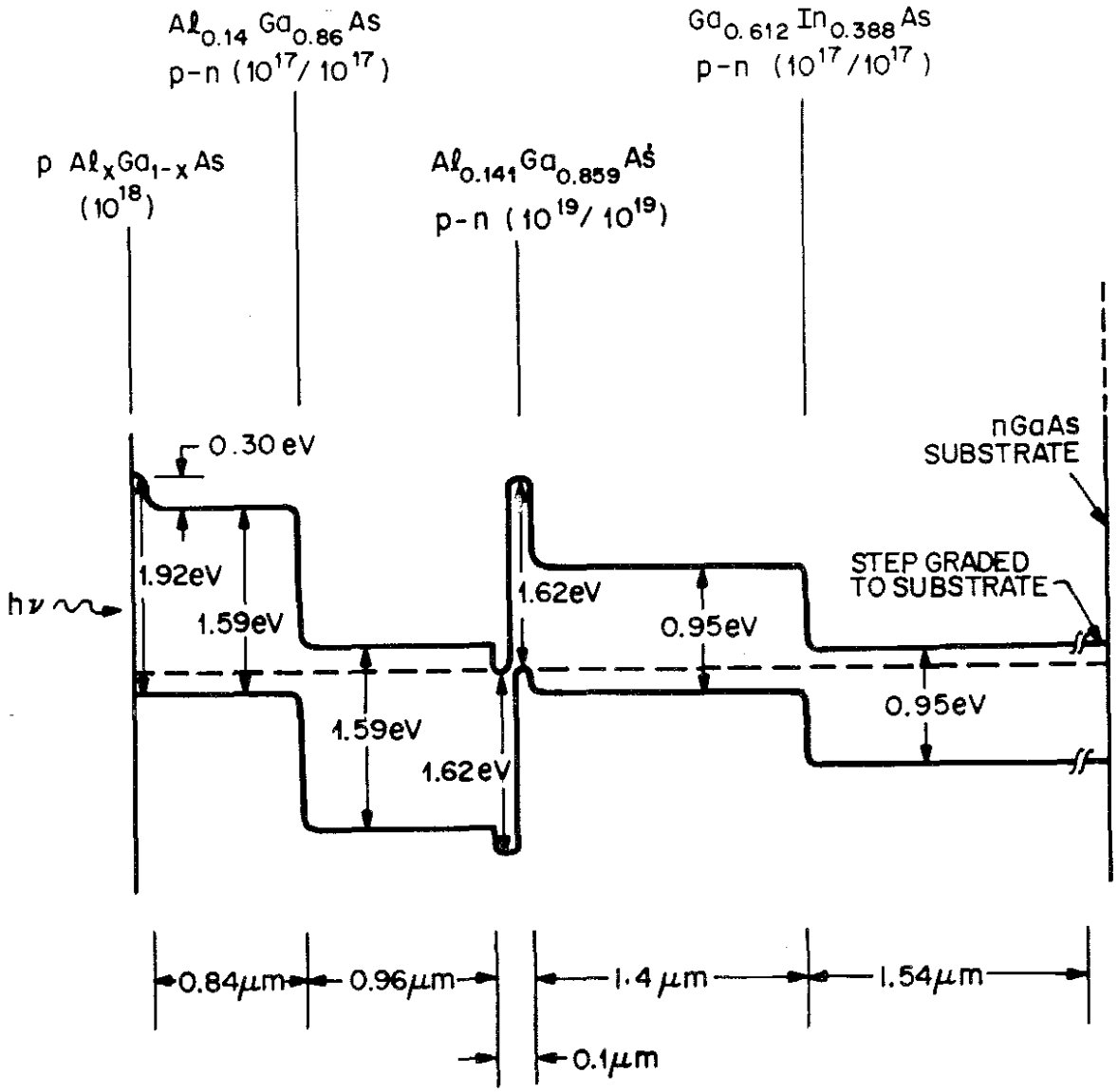

Fig. 25 An idealized cascade two-junction solar cell. (After Lamorte and Abbott, Ref. 31.)

SM Sze, Physics of Semiconductor Devices, 2nd ed.

Metal-semiconductor –Schottky barrier solar cells

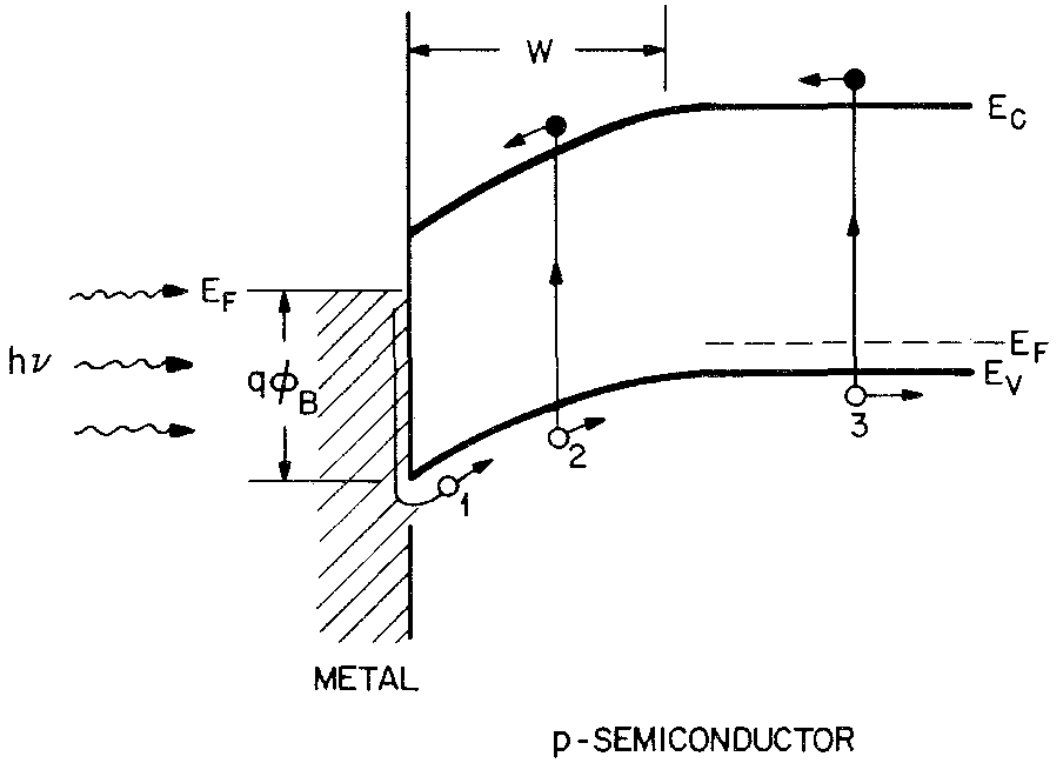

Fig. 26 Energy-band diagram of a Schottky-barrier solar cell under illumination.

SM Sze, Physics of Semiconductor Devices, 2nd ed.

Amorphous Silicon Solar Cells

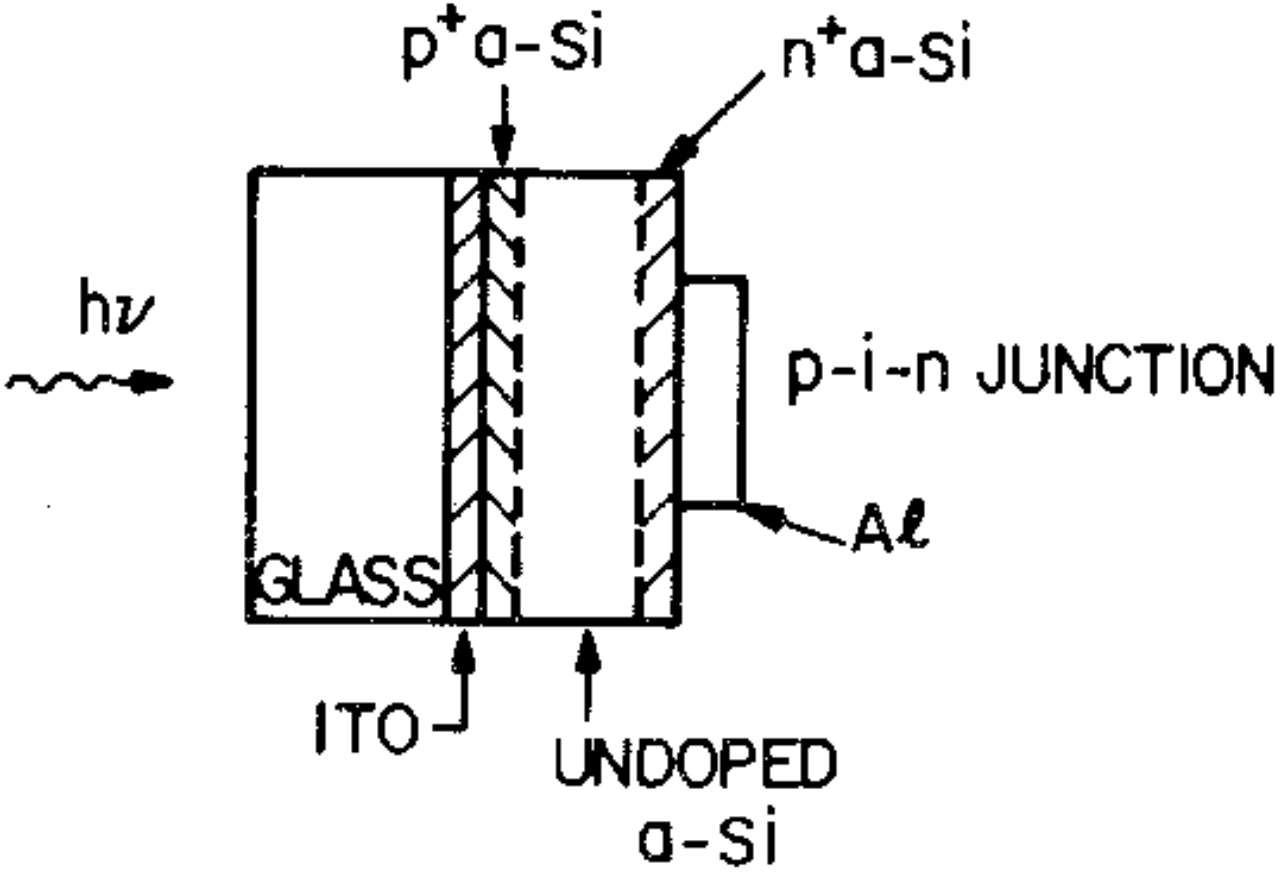

SM Sze, Physics of Semiconductor Devices, 2nd ed.

Concentrator solar cells

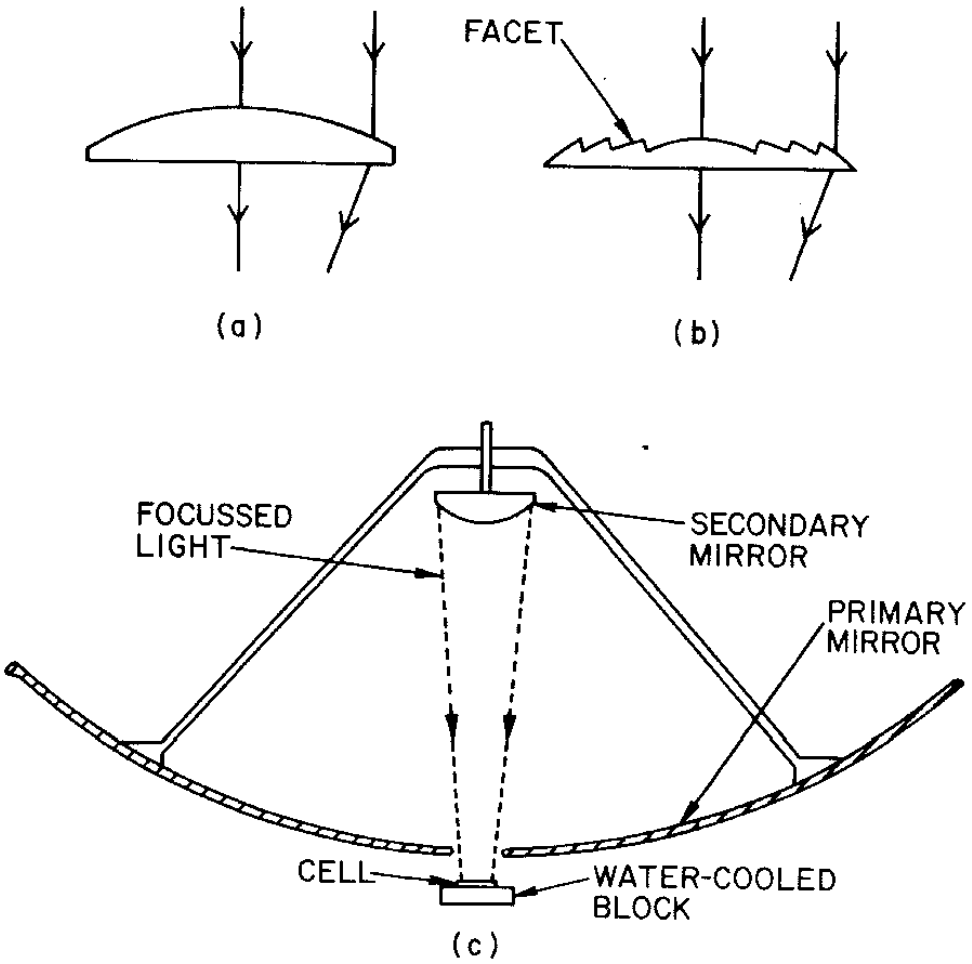

Fig. 37 (a) Standard lens. (*b*) Fresnel lens. (*c*) Typical concentrator module.

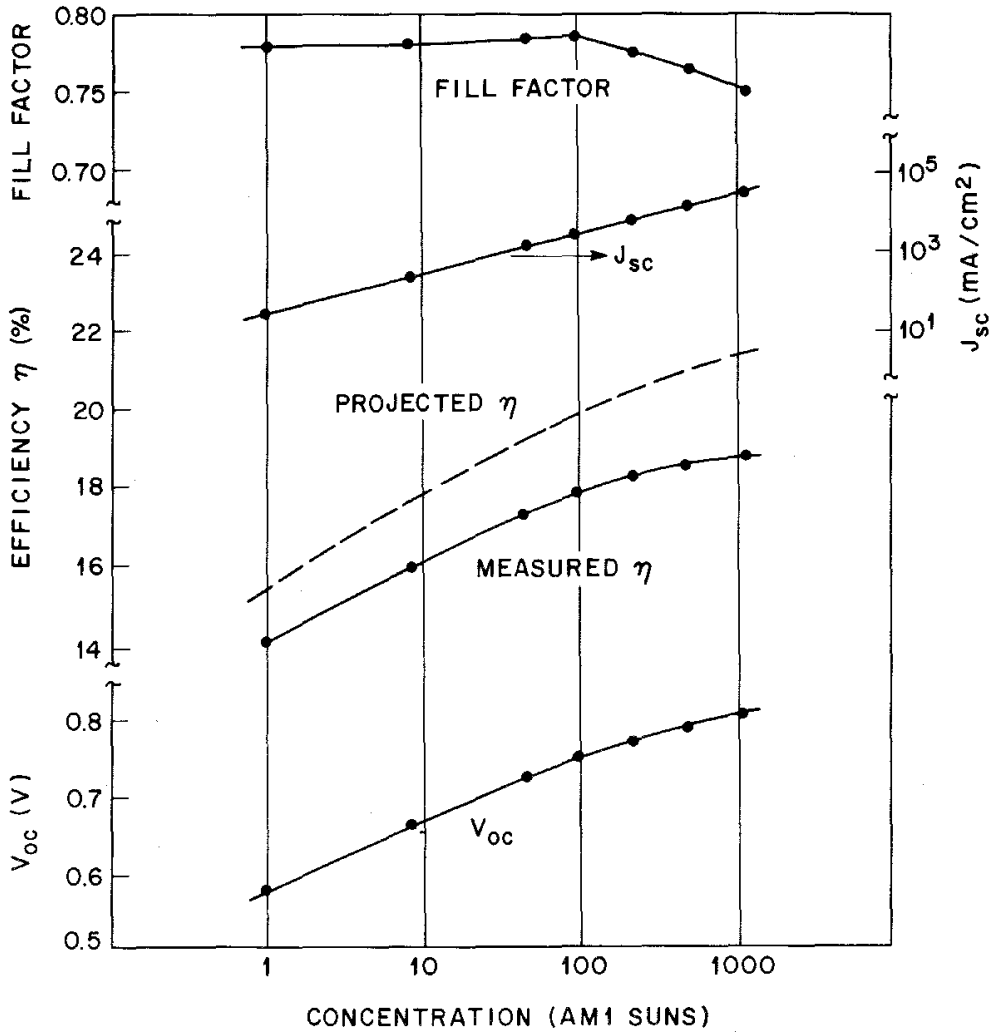

Fig. 38 Efficiency, V_{oc}, J_{sc}, and fill factor versus AM1 solar concentration for a multiple vertical junction. (After Frank, Goodrich, and Kaplow, Ref. 44.)

Solar cells with a spectral-splitting arrangement

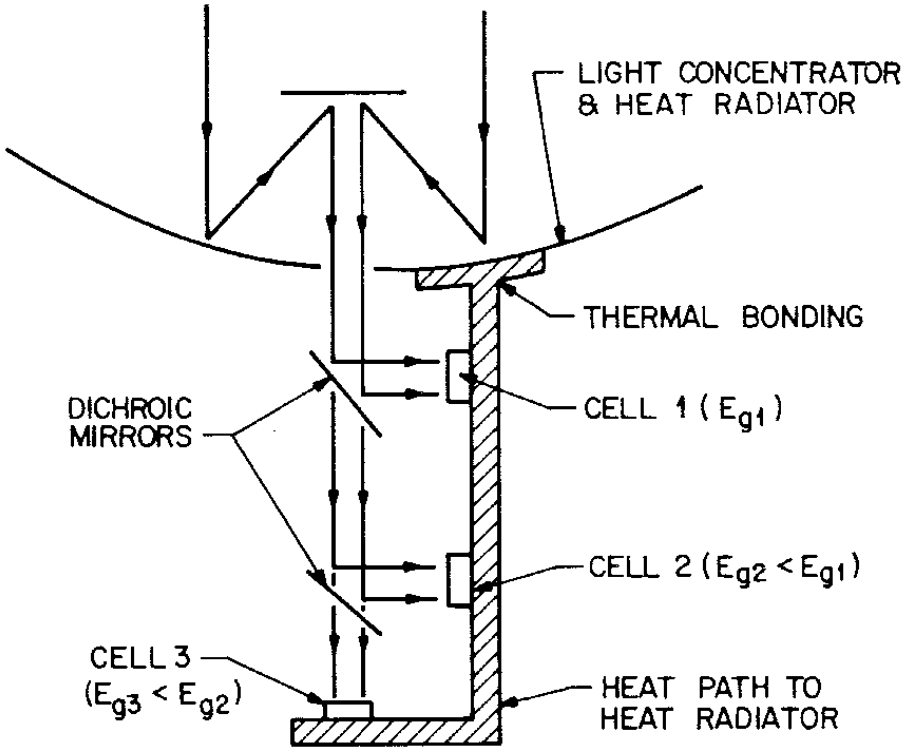

Fig. 41 Possible module design of spectral splitting for high-efficiency operation. (After Blocker, Ref. 46.)

SM Sze, Physics of Semiconductor Devices, 2nd ed.

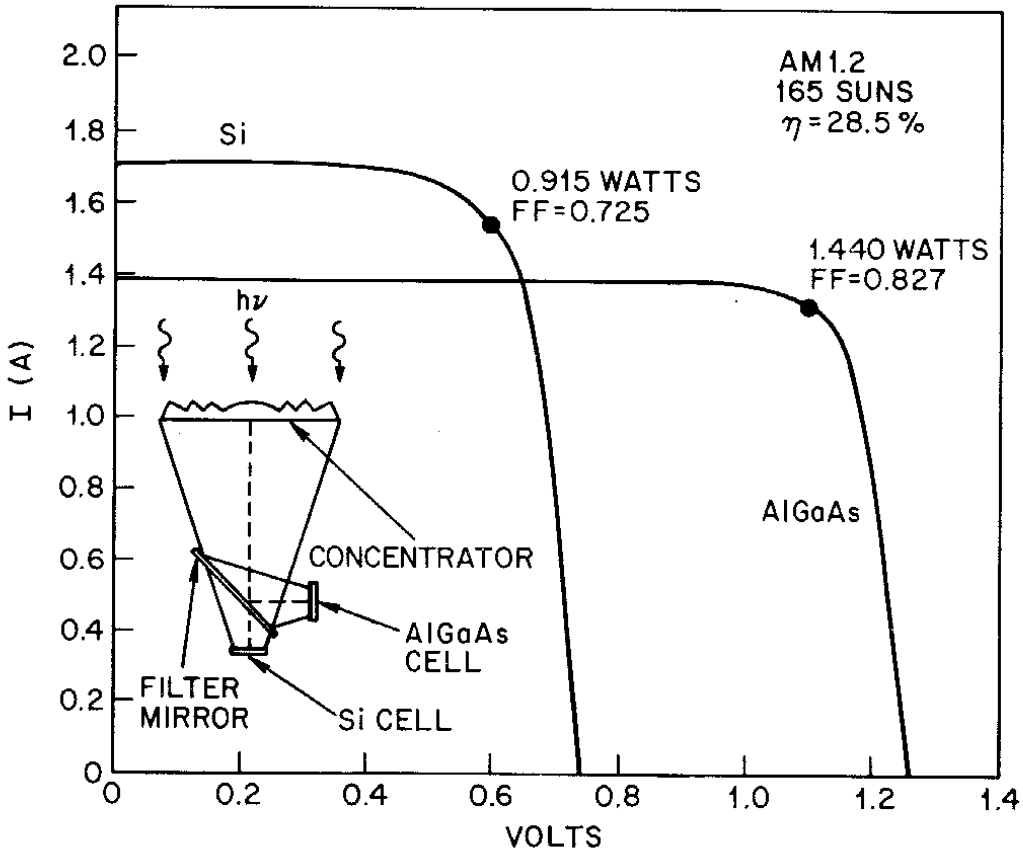

Fig. 42 Current–voltage curves for Si and AlGaAs solar cells in a spectral-splitting arrangement, operating under 165 suns. (After Moon et al., Ref. 47.)

Luminescent concentrators

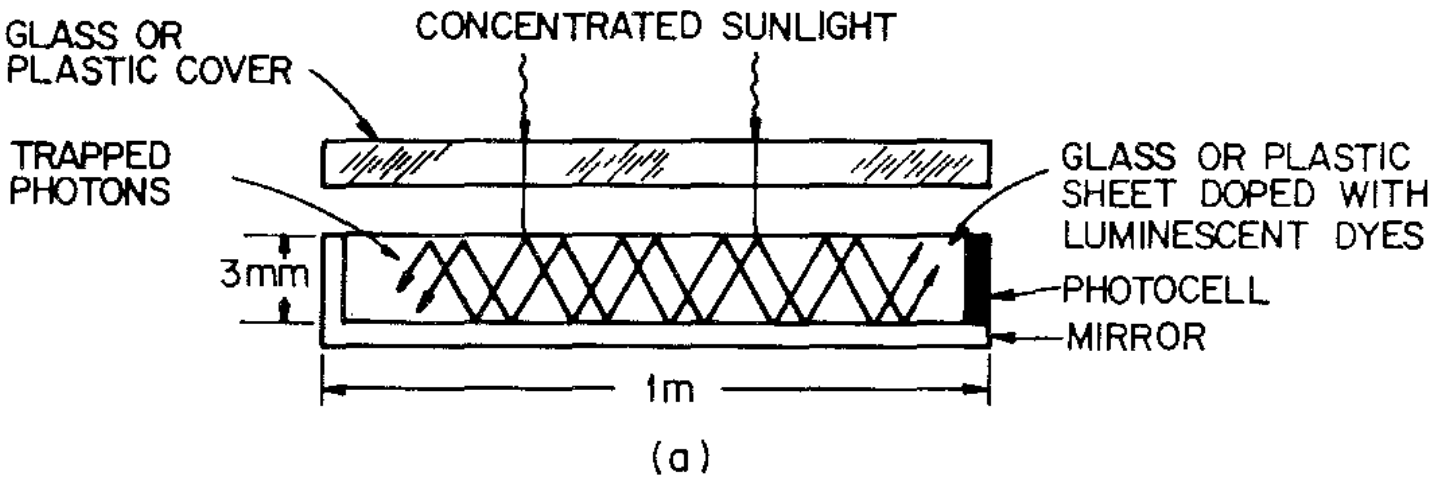

SM Sze, Physics of Semiconductor Devices, 2nd ed.

Organic solar cells

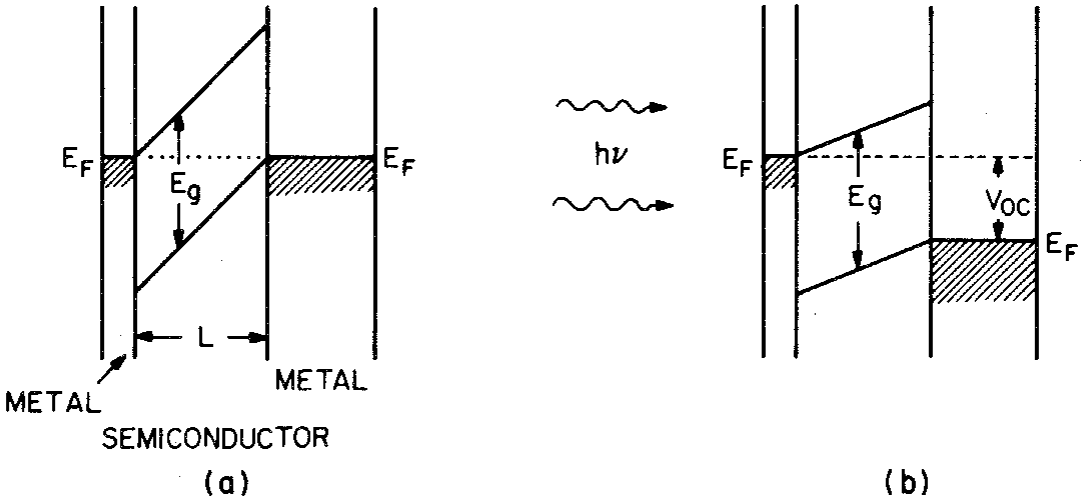

Fig. 36 Idealized configuration for a thin-film cell (*a*) in dark equilibrium and (*b*) under illumination. (After Ref. 13.)

SM Sze, Physics of Semiconductor Devices, 2nd ed.

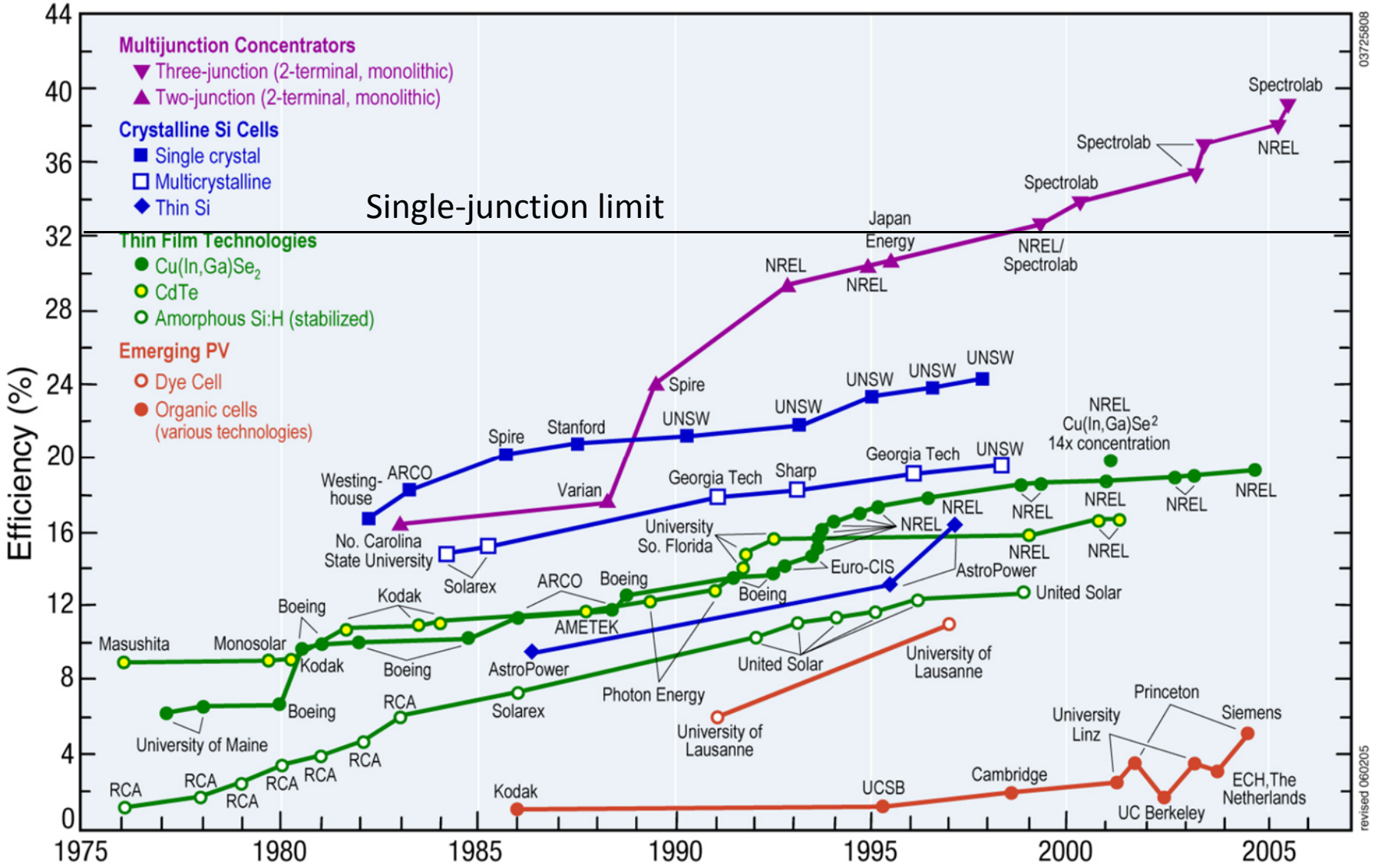

Figure 3 Improvements in solar cell efficiency, by system, from 1976 to 2004

DOE_BES report - http://www.sc.doe.gov/bes/reports/files/SEU_rpt.pdf.